

# SINEUP Non-coding RNA Targeting GDNF Rescues Motor Deficits and Neurodegeneration in a Mouse Model of Parkinson's Disease

Stefano Espinoza,<sup>1</sup> Margherita Scarpato,<sup>1</sup> Devid Damiani,<sup>1</sup> Francesca Managò,<sup>1</sup> Maddalena Mereu,<sup>1,2</sup> Andrea Contestabile,<sup>1</sup> Omar Peruzzo,<sup>1</sup> Piero Carninci,<sup>3</sup> Claudio Santoro,<sup>4</sup> Francesco Papaleo,<sup>1</sup> Federico Mingozzi,<sup>5</sup> Giuseppe Ronzitti,<sup>5</sup> Silvia Zucchelli,<sup>4,6</sup> and Stefano Gustincich<sup>1</sup>

<sup>1</sup>Central RNA Laboratory and Department of Neuroscience and Brain Technologies, Istituto Italiano di Tecnologia (IIT), 16263 Genova, Italy; <sup>2</sup>Dipartimento di Scienze del Farmaco, Università degli Studi di Padova, Largo Meneghetti 2, 35131 Padova, Italy; <sup>3</sup>RIKEN Center for Life Science Technologies, Division of Genomic Technologies, Yokohama, Kanagawa, Japan; <sup>4</sup>Department of Health Sciences and Interdisciplinary Research Center of Autoimmune Diseases (IRCAD), University of Piemonte Orientale (UPO), 28100 Novara, Italy; <sup>5</sup>INTEGRARE, Genethon, Inserm, Univ Evry, Université Paris-Saclay, 91002 Evry, France; <sup>6</sup>Area of Neuroscience, Scuola Internazionale degli Studi Avanzati (SISSA), 34012 Trieste, Italy

**Glial cell-derived neurotrophic factor (GDNF) has a potent action in promoting the survival of dopamine (DA) neurons. Several studies indicate that increasing GDNF levels may be beneficial for the treatment of Parkinson's disease (PD) by reducing neurodegeneration of DA neurons. Despite a plethora of preclinical studies showing GDNF efficacy in PD animal models, its application in humans remains questionable for its poor efficacy and side effects due to its uncontrolled, ectopic expression. Here we took advantage of SINEUPs, a new class of antisense long non-coding RNA, that promote translation of partially overlapping sense protein-coding mRNAs with no effects on their mRNA levels. By synthesizing a SINEUP targeting *Gdnf* mRNA, we were able to increase endogenous GDNF protein levels by about 2-fold. Adeno-associated virus (AAV) 9-mediated delivery in the striatum of wild-type (WT) mice led to an increase of endogenous GDNF protein for at least 6 months and the potentiation of the DA system's functions while showing no side effects. Furthermore, SINEUP-GDNF was able to ameliorate motor deficits and neurodegeneration of DA neurons in a PD neurochemical mouse model. Our data indicate that SINEUP-GDNF could represent a new strategy to increase endogenous GDNF protein levels in a more physiological manner for therapeutic treatments of PD.**

## INTRODUCTION

Parkinson's Disease (PD) is one of the most common neurodegenerative disorders, and it is caused by loss of the dopamine (DA) neurons of the substantia nigra pars compacta (SNpc). It manifests its symptomatology mainly as motor-related deficits, such as rigidity, tremor, and bradykinesia.<sup>1</sup> Although familial PD (about 5% of the total cases) has been important to unveil the molecular pathways involved in neurodegeneration, most of the PD patients are sporadic.<sup>2</sup> Currently, no treatments are available that can slow or arrest neurodegeneration. The DA precursor L-DOPA is the gold standard for symptomatic

treatments, although over time it may lead to several side effects and resistance.<sup>3</sup>

Glial cell-derived neurotrophic factor (GDNF) is the most potent neurotrophic factor for DA neurons with great potentiality for clinical application.<sup>4,5</sup> GDNF can protect DA cells and promotes their survival from toxic insults *in vitro* and *in vivo* in mice, rats, and non-human primates.<sup>6–8</sup> However, clinical trials with recombinant GDNF showed an inconsistency of results, due to the poor spreading of GDNF within the parenchyma and to the unsustainable side effects caused by the high doses of GDNF administered.<sup>9–11</sup> Similarly, GDNF expression through viral vectors that showed efficacy in PD animal models may result in uncontrolled, ectopic GDNF overexpression. Therefore, GDNF may be the right candidate for PD therapy, provided that a more specific and physiological expression is achieved to increase its efficacy and safety profile *in vivo*. In this context, a deletion in the 3' UTR of the *GDNF* gene in a transgenic mouse line led to an increase of 2-fold of endogenous GDNF protein levels.<sup>12</sup> This was sufficient to induce alterations in the DA system and neuroprotection similar to what was seen with a large overexpression of GDNF, but without the side effects. These data corroborate the hypothesis that a moderate increase in endogenous GDNF could be beneficial for PD.

We have previously identified antisense (AS) *Uchl1* as a long non-coding RNA (lncRNA) antisense to mouse *Uchl1/Park5* that increases *Uchl1* protein synthesis at the post-transcriptional level.<sup>13</sup> AS *Uchl1* is the representative member of a new functional class of natural and synthetic lncRNAs, named SINEUPs, that promote translation of

Received 25 March 2019; accepted 12 August 2019;  
<https://doi.org/10.1016/j.ymthe.2019.08.005>.

**Correspondence:** Stefano Gustincich, Central RNA Laboratory and Department of Neuroscience and Brain Technologies, Istituto Italiano di Tecnologia (IIT), via Morego 30, Genova 16263, Italy.

**E-mail:** [stefano.gustincich@iit.it](mailto:stefano.gustincich@iit.it)



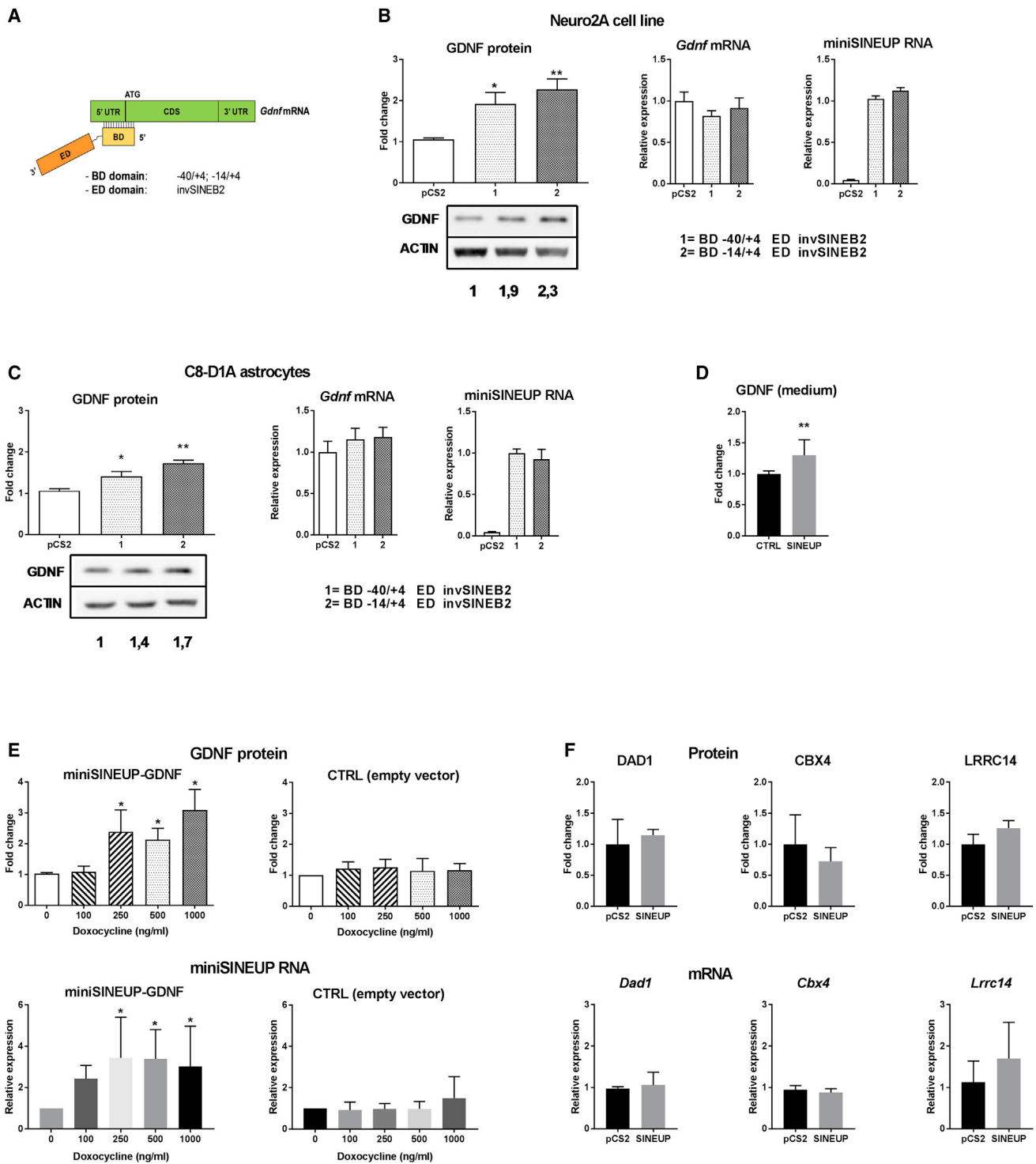


**Figure 1. *miniSINEUP-GDNF* RNA Increases Selectively GDNF Protein Expression In Vitro**

(A) Schematic representation of *miniSINEUP-GDNF* structure, with the SINEUP BD overlapping the 5' UTR of the *Gdnf* mRNA. (B and C) Effect of *miniSINEUP-GDNF* RNA on endogenous GDNF protein levels in two cell lines, the Neuro2a (B) and the C8-D1A astrocytes (C) ( $F_{2, 12} = 8.09$ ,  $p < 0.001$ ,  $n = 5$  for Neuro2a; and  $F_{2, 9} = 15.69$ ,  $p < 0.01$ ,  $n = 4$  for astrocytes). *miniSINEUP-GDNF* transfected in cells increases GDNF proteins levels without altering *Gdnf* mRNA levels. Both *miniSINEUP* RNA with two different BD (-40/+4 and the -14/+4, respectively) were expressed in transfected cells, but not in CTRL cells. (D) *miniSINEUP-GDNF* increases extracellular GDNF secreted by cells, as

(legend continued on next page)

partially overlapping sense protein-coding mRNAs with no effects on their mRNA levels.<sup>14</sup> SINEUPs' activity depends on the combination of two domains: the overlapping region or binding domain (BD), which dictates SINEUP specificity, and the embedded inverted SINEB2 element, which acts as the effector domain (ED) controlling the enhancement of mRNA translation. Their modular structure can be employed to artificially engineer their BD and design synthetic SINEUPs to specifically enhance translation of virtually any target gene of interest. miniSINEUP RNAs are exclusively composed by ED and BD sequences.

Synthetic SINEUPs and miniSINEUPs have been proven effective with a number of targets, including GFP, FLAG-tagged proteins, and secreted recombinant antibodies and cytokines, thus showing SINEUP technology is scalable.<sup>15–17</sup> Furthermore, SINEUPs can act on endogenous mRNAs *in vitro* and *in vivo*. In a Medaka fish model of microphthalmia with linear skin lesions and in a cellular model of Friedreich ataxia, SINEUPs increased endogenous protein levels of, respectively, *Cox7b* and *frataxin*, restoring eye development *in vivo* and physiological mitochondria activity in patients' cells.<sup>18</sup> These results suggest the use of SINEUP technology in treating haploinsufficiencies where a single functional allele is not sufficient to encode for physiological amounts of the protein. In a parallel strategy, SINEUPs may be used to increase the expression of neuroprotective agents to compensate for a disease phenotype.

Here we have designed and successfully tested miniSINEUP RNAs specific for GDNF (*miniSINEUP-GDNF*) that selectively induced GDNF protein levels *in vitro*. We then proved that these non-coding RNAs are able to stably increase GDNF protein levels in the mouse striatum. Finally, *miniSINEUP-GDNF* was able to ameliorate motor deficits and DA neurodegeneration in mice unilaterally lesioned with 6-hydroxy-dopamine (6-OHDA).

These results may pave the way to a new strategy for increasing endogenous GDNF in PD therapy and to the establishment of a novel, RNA-based therapeutic platform to address genetic and idiopathic diseases.

## RESULTS

### miniSINEUP-GDNF RNA Selectively Increases GDNF Protein Expression *In Vitro*

To design a specific SINEUP for endogenous *Gdnf* mRNA, we first evaluated transcription start site (TSS) usage in cells and tissues relevant for PD. We thus interrogated the FANTOM5 collection of Cap Analysis of Gene Expression (CAGE) datasets, which represents the widest catalog of annotated promoters and TSSs in mammalian sam-

ples.<sup>19</sup> By using the Zenbu Genome Browser Tool for data visualization,<sup>20</sup> we monitored TSS usage at the mouse GDNF locus and evaluated their expression in a variety of samples. The main TSS was close to the first ATG, suggesting that the first two annotated isoforms (NM\_001301332.1 and NM\_010275.3) were the most widely expressed (Figure S1).

Based on this TSS analysis, we designed two GDNF-specific miniSINEUPs (*miniSINEUP-GDNF*) in antisense orientation to *Gdnf* mRNA around the first AUG, following the rules of pairing at the sense (S)/AS Uchl1 locus<sup>13</sup> and for other natural and synthetic SINEUPs.<sup>14</sup> While they presented the very same, original ED from the SINEB2 sequence of mouse AS Uchl1 RNA, two different BD sequences were synthesized: a long one (–40/+4) and a short one (–14/+4), giving rise to *miniSINEUP-GDNFs* of around 250 nt in length (Figure 1A).

To test *miniSINEUP-GDNF* efficacy, we took advantage of two mouse cell lines that express endogenous *Gdnf* mRNA,<sup>21</sup> the neuroblastoma Neuro2a and the astrocyte C8-D1A cell lines, verifying first that *Gdnf* mRNA was present (Figure S2). SINEUP activity was evaluated by measuring GDNF protein levels by western blot. Their post-transcriptional control of target gene expression was monitored with qRT-PCR. Both SINEUPs demonstrated a significant activity (Figures 1B and 1C), with the one with the short BD (–14/+4) being the more active (2.3- and 1.7-fold increases in Neuro2a and C8, respectively) compared to the *miniSINEUP-GDNF* with the longest BD (1.9- and 1.4-fold increases in Neuro2a and C8, respectively). Both SINEUPs did not show any effect at the transcriptional level, with no change in *Gdnf* mRNA (Figures 1B and 1C).

Since GDNF is released outside cells and its secretion confers neuroprotection of the DA terminals in the striatum, we measured secreted GDNF protein levels in the medium of C8 astrocytes 2 days from *miniSINEUP-GDNF* transfection. As shown in Figure 1D, *miniSINEUP-GDNF* (–14/+4) increased secreted GDNF protein levels by about 40%. We then cloned *miniSINEUP-GDNFs* in a pLVX-TetOne vector under the control of a doxocycline-inducible promoter. miniSINEUP RNA levels reached a plateau at 250 ng/mL, corresponding to its peak activity (Figure 1E).

SINEUP specificity is given by the BD nucleotide sequence that is unique for the endogenous mRNA target. However, like other nucleic acid-based techniques, off-targets cannot be excluded. Thus, we took advantage of the BLAST to predict potential off-targets, aligning the BD sequence to the mouse mRNA dataset. Three off-target candidates showed the highest sequence similarity: *Dad1* (homologous on the 3' UTR, 15 nt of similarity), *Lrrc14* (homologous in the coding

---

measured by an ELISA (n = 8). (E) Neuro2a cells were transfected with a pLVX-TetOne vector expressing the *miniSINEUP-GDNF*. After 24 h post-transfection, cells were treated with different concentrations of doxocycline for 24 h to evaluate the correlation between miniSINEUP RNA levels and GDNF protein expression. The induction of the *miniSINEUP-GDNF* RNA expression by doxocycline ( $F_{4, 29} = 3.45$ ,  $p < 0.05$ ) provokes an increase in GDNF protein levels ( $F_{4, 20} = 3.52$ ,  $p < 0.05$ ,  $n = 3$ ). (F) Off-target effects of *miniSINEUP-GDNF* were studied. After a BLAST analysis, the protein and mRNA levels of three possible off-targets were measured with western blot and qRT-PCR, namely, DAD1, CBX4, and LRRC14. *miniSINEUP-GDNF* did not alter protein or mRNA levels of these potential off-targets (n = 3). Data represent means  $\pm$  SEM. \* $p < 0.05$ , \*\* $p < 0.01$ , \*\*\* $p < 0.001$ . Unpaired t test with Welch's correction (D and F) or one-way ANOVA followed by Dunnett's multiple comparison test was used (B, C, and E).

sequence, 14 nt of similarity), and *Cbx4* (homologous on the 3' UTR, 17 nt of similarity) (Table S1). As shown in Figure 1F, *miniSINEUP-GDNF* did not alter the protein or mRNA levels of these genes, proving the specificity of activity. To further demonstrate the on-target effects of *miniSINEUP-GDNF*, we produced a *miniSINEUP* lacking the BD (*deltaBD-miniSINEUP-GDNF*), to eliminate the specificity for the endogenous *Gdnf* mRNA. Importantly, *deltaBD-miniSINEUP-GDNF* had no effects on GDNF protein levels compared to *miniSINEUP-GDNF* (Figure S3).

#### AAV9-Mediated Delivery of *miniSINEUP-GDNF* RNA Increases Endogenous GDNF Expression in the Mouse Striatum

To test the functionality of the *miniSINEUP-GDNF* *in vivo*, we designed an AAV9 vector to express SINEUP RNA under the control of the cytomegalovirus (CMV) early enhancer/chicken beta-actin (CAG). Since we couldn't produce an AAV with two CAG promoters, we used another ubiquitous promoter, the phosphoglycerate kinase (PGK), to drive the expression of GFP, although its expected activity in astrocytes is lower (Figure 2A). Using this vector, *miniSINEUP-GDNF* maintained its GDNF protein upregulation activity when tested *in vitro* in Neuro2a and C8 astrocytes (Figure 2B). AAV9 vectors expressing *miniSINEUP* RNA and the empty vector (CTRL) were produced and stereotaxically injected into the dorsal striatum of adult C57BL/6J mice at the dose of  $7.0 \times 10^9$  vector genomes (vg) per site of injection.

At 5 weeks post-infection, transgenes were widely expressed in the majority of neurons of the dorsal striatum (Figure 2C). As expected, PGK promoter was more effective in expressing GFP in neuronal than in glial cells. We also noted some GFP-positive cells outside the area, especially close to the ventricle, probably due to leaking of the virus. Most importantly, *miniSINEUP-GDNF* increased GDNF protein levels by about 80% (Figure 2D), an effect comparable to the one seen *in vitro* in cell lines. RNA expression and SINEUP activity were maintained up to 6 months after vector administration (Figure 2E). These results prove a stable expression of the transgene and a continuous increase in endogenous GDNF protein levels.

#### Striatal GDNF Is Functionally Active *In Vivo* When Synthesized through a *miniSINEUP-GDNF*-Dependent Mechanism

Overexpression of GDNF in the striatum using viruses or the recombinant protein leads to several consequences, including an alteration of the DA system's functions.<sup>22</sup> To test whether the increase in GDNF protein levels achieved by *miniSINEUP-GDNF* RNA was functionally relevant, we first injected mice with amphetamine, a DA reuptake inhibitor that stimulates locomotion. Interestingly, mice injected with *AAV9-miniSINEUP-GDNF* were more sensitive to the stimulating effects of amphetamine (Figure 3A). We then used *in vivo* microdialysis to evaluate DA release in the striatum injected with *miniSINEUP-GDNF* RNA. As shown in Figure 3B, DA basal levels were not changed. However, when DA release was stimulated by the infusion of potassium or amphetamine, mice with *miniSINEUP-GDNF* RNA showed an enhanced DA release compared to CTRL animals (Figures 3C and 3D). This effect was likely due to an increase in DA storage in the terminals, since we found an increase in DA total content in the

striatum of mice injected with *AA9-miniSINEUP-GDNF*, although a higher number of DA cells' terminals cannot be excluded (Figure 3E).

Uncontrolled ectopic expression of GDNF has led to several side effects in mice and in humans during clinical trials, including an increase in basal locomotor activity and reduced body weight and food intake.<sup>4,12</sup> Here we showed that, 4 months after vector injection, mice expressing *miniSINEUP-GDNF* RNA did not show any alteration of locomotor parameters (Figure 3F), body weight (Figure 3G), and food intake (Figure 3H). These results prove that the SINEUP-mediated increase in GDNF occurs within a physiological range, without triggering any deleterious effects *in vivo*.

#### *miniSINEUP-GDNF* RNA Rescues Neurodegeneration and Motor Phenotype in a PD Neurochemical Mouse Model

We then tested whether *miniSINEUP-GDNF* RNA was effective as a neuroprotective agent in a PD neurochemical mouse model. To this purpose, we stereotaxically injected *AAV9-miniSINEUP-GDNF* or the CTRL virus into the striatum and induced 6-OHDA unilateral lesions 4 weeks later (Figure 4A). No evident signs of cortical damage were induced by the two surgeries (Figure S4). 6-OHDA was able to induce lesions of DA terminals, as previously shown by many studies (Figure 4B).

At 6 weeks after the intoxication and 10 weeks after AAV injections, we carried out a battery of behavioral tests. First, we performed the cylinder test to assess the motor functionality of the forepaw, since it is well known to be impaired in lesioned mice. Mice with *miniSINEUP-GDNF* RNA showed an increase in contralateral touches and a parallel decrease in ipsilateral touches, indicating a recovery of the forepaw that was under the control of the lesioned striatum (Figure 4C). Then, we scored the mice for rotations, a sign of the severity of the lesion. Both spontaneous rotations and those induced by amphetamine were strongly reduced in mice with *miniSINEUP-GDNF* RNA (Figure 4D), suggesting that *miniSINEUP-GDNF* was able to reduce striatal neurodegeneration.

To verify this interpretation, we evaluated the quantity of DA terminals in the lesioned striatum by measuring tyrosine hydroxylase (TH) immunoreactivity. As shown in Figure 4E, mice injected with *miniSINEUP-GDNF* showed an increase in TH staining and a reduction in the lesion induced by 6-OHDA intoxication. Furthermore, mice with *miniSINEUP-GDNF* RNA showed an increase in TH-positive neurons in the SNpc with a recovery of the lesion of about 50% (Figure 4F). To verify that the enhancement of GDNF protein levels was present under pathological conditions, we carried out the very same protocol of sequential viral injection and lesion with 6-OHDA in another cohort of mice. As shown in Figure S5, mice injected with *AAV-miniSINEUP-GDNF* presented higher levels of GDNF in the striatum after 1 month from the time of lesion.

#### DISCUSSION

Nucleic acid-based therapy has been constantly developing in the last years, with several drug candidates in clinical development for human



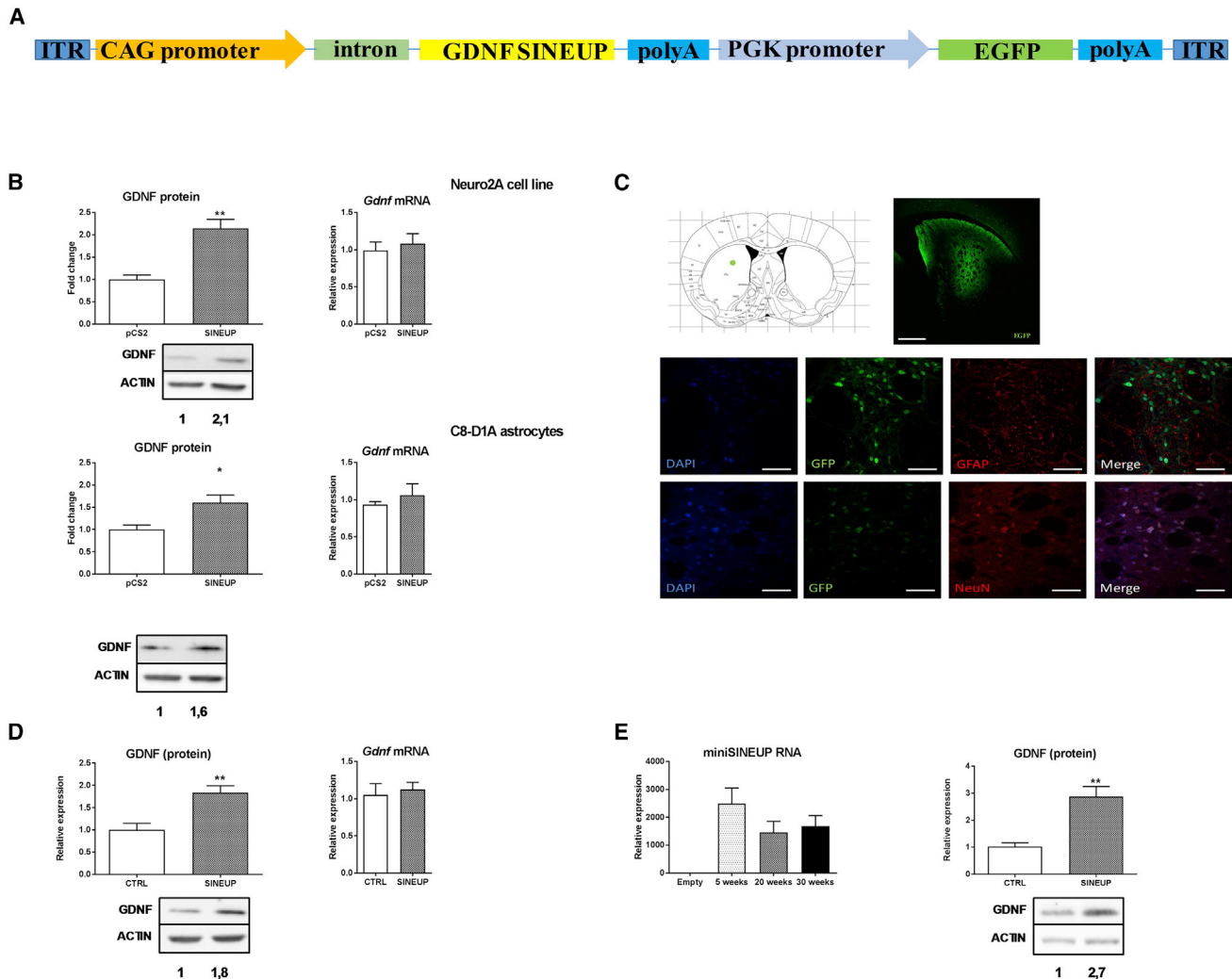


**Figure 2. AAV9-Mediated Delivery Expression of *miniSINEUP-GDNF* RNA Increases Endogenous GDNF Expression in the Mouse Striatum**

(A) Schematic representation of the modified AAV9 vector used to express the *miniSINEUP-GDNF* and GFP as a reporter. (B) AAV9 plasmid was transfected in Neuro2a and astrocytes cell lines to test the expression of *miniSINEUP-GDNF*. In both cell lines, GDNF protein levels were increased with no alteration of *Gdnf* mRNA levels ( $n = 3$ ). (C) AAV9 viral particles were stereotactically injected in the right dorsal striatum of C57BL/6J mice and GFP expression was studied with a fluorescent microscope. Co-localization immunofluorescence was performed to evaluate GFP expression. NeuN was used to stain neurons and GFAP to stain astrocytes. Most of the GFP (expressed under PGK promoter) was present in neurons. Scale bars, 250  $\mu\text{m}$  upper panel and 50  $\mu\text{m}$  lower panels. (D) At 5 weeks after viral injection, striata were dissected and GDNF protein levels were evaluated with western blot. Mice injected with the AAV9-*miniSINEUP-GDNF* showed an increase in GDNF protein levels ( $n = 6$  for CTRL mice and 7 for *miniSINEUP-GDNF* mice). (E, left panel) *miniSINEUP* RNA expression levels at different time points after viral injection. Mice injected with the virus were dissected at 5, 20, and 30 weeks post-injection. *SINEUP* RNA was present at high levels up to 30 weeks ( $n = 7, 5,$  and 5 for each time point, respectively). (E, right panel) Effect of AAV9-*miniSINEUP-GDNF* on GDNF protein levels at 30 weeks post-injection. Mice injected with AAV9-*miniSINEUP-GDNF* showed an increase in GDNF protein levels ( $n = 6$  for CTRL mice and 5 for *miniSINEUP-GDNF* mice). Data represent means  $\pm$  SEM. \* $p < 0.05$ , \*\* $p < 0.01$ , \*\*\* $p < 0.001$ . Unpaired t test with Welch's correction was used.

diseases.<sup>23</sup> Generally, RNAs act as inhibitory molecules and most of them are small interfering RNAs (siRNAs) and AS oligonucleotides (ASOs). On the other hand, molecules able to increase the expression of selected genes would be of great interest for the treatment of several pathologies. To this purpose, transcriptional activating RNAs and non-degradative ASOs have been recently used *in vitro* and in *in vivo* disease models.<sup>24–26</sup>

In this study, we demonstrate that SINEUPs, non-coding RNAs that activate the translation of target mRNAs, can be used as a novel tool for gene therapy. As a proof of concept, we designed a SINEUP targeting endogenous *Gdnf*, and we proved that *miniSINEUP-GDNF* RNA is effective in increasing GDNF protein levels *in vivo* and in rescuing motor symptoms and neurodegeneration in a PD mouse model.

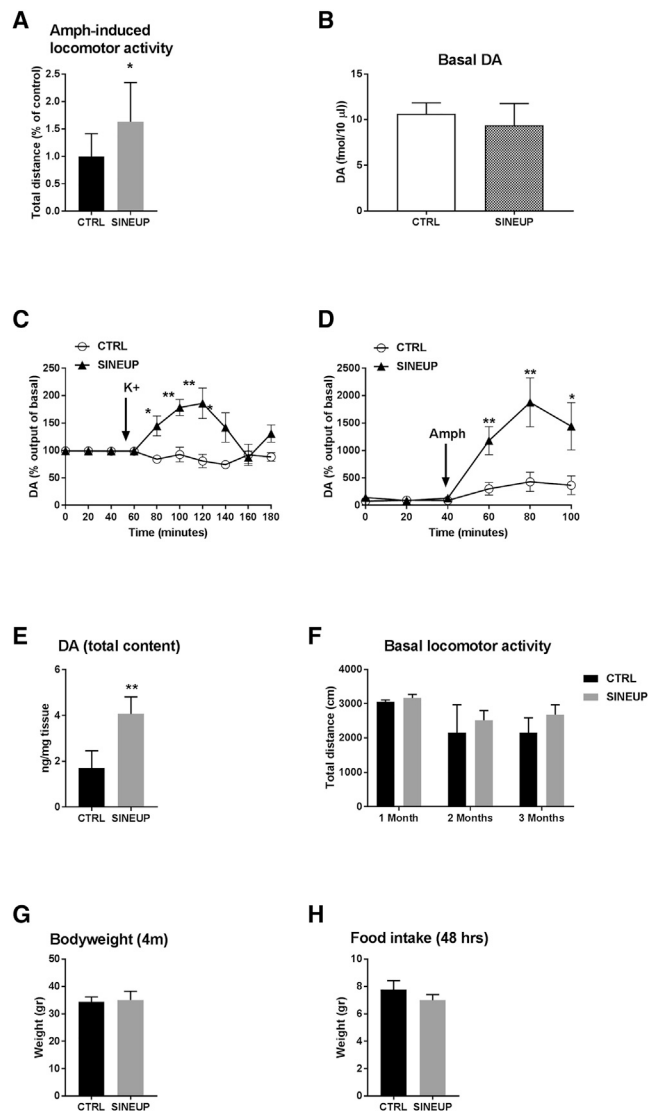


**Figure 3. Striatal GDNF Is Functionally Active *In Vivo* When Synthesized through a *miniSINEUP-GDNF*-Dependent Mechanism**

(A) Mice, 4 months after AAV9-*miniSINEUP-GDNF* injection, were put in locomotor chambers, injected with amphetamine at 2.5 mg/kg, and locomotor activity was measured. Mice injected with AAV9-*miniSINEUP-GDNF* showed an increase in locomotor activity ( $n = 12$ ). (B) Extracellular DA release was measured in the striatum of mice injected with AAV9-*miniSINEUP-GDNF*, 4 months after injection. *In vivo* microdialysis was performed to collect samples from the striatum, and DA was measured using a high-performance liquid chromatography (HPLC) system. Basal DA level was not changed between SINEUP and CTRL groups. After depolarization of DA terminals by reverse microdialysis infusion of (C) potassium 120 nM or (D) amphetamine 250  $\mu$ M in the artificial cerebrospinal fluid (ACSF) solution, mice injected with AAV9-*miniSINEUP-GDNF* showed an increase in DA extracellular levels (treatment\*mouse  $F_{3, 40} = 4.84$ ,  $p < 0.001$ ,  $n = 4$ ). (E) Total striatal DA content was measured from animals injected with AAV9-*miniSINEUP-GDNF* or CTRL virus. Mice injected with AAV9-*miniSINEUP-GDNF* showed an increase in striatal DA total content ( $n = 5$ ). (F) Locomotor activity in mice injected with AAV9 vector was measured at different time points after the injection. Total distance traveled by the two groups of animals was evaluated for 3 months ( $n = 8$ ). (G and H) Two different

GDNF was cloned almost 30 years ago, and several experimental studies in rodents and non-human primates have been demonstrating that increasing GDNF levels is beneficial for the survival of DA neurons.<sup>4-7</sup> However, clinical trials in humans with GDNF recombinant protein did not give straightforward results, showing promising improvements but also a lack of efficacy and unsustainable side effects. Major problems concern the large excess of the protein, way above physiological levels, and its poor spreading in the tissue.<sup>9,11</sup> Despite a good efficacy in preclinical PD models, GDNF overexpression with viral vectors, either lentivirus or AAV, has showed similar side effects and limitations.<sup>4</sup> This is possibly due to the uncontrolled overexpression of the transgene occurring above physiological levels. Side effects and poor efficacy also can be caused by unspecific, ectopic expression of the transgene in cells that normally do not present it. While it is sometimes possible to drive transgene expression in the correct cells with specific promoters, the repertoire of human neuronal cell type-specific promoters is very limited or they are often too large to be included in a viral vector. GDNF expression in the striatum is restricted to parvalbumin GABAergic interneurons, but the viral vectors used to overexpress GDNF so far always contained ubiquitous promoters.

Here we show that both *in vitro* and *in vivo miniSINEUP-GDNF* increases GDNF protein levels by about 2-fold. This is in line with SINEUPs we and others developed, measuring upregulation of the target protein in a range of 1.5- to 4-fold induction.<sup>14,16</sup> As previously shown in genetically modified mice,<sup>12</sup> this moderate increase is sufficient to physiologically modulate endogenous DA systems preventing side effects.

The active *miniSINEUP-GDNF* has a BD of 18 nt that specifically pairs with endogenous *Gdnf* mRNA isoforms. Therefore, SINEUPs act only in cells that express the target mRNA. Since all nucleotide-based approaches, including those based on the CRISPR-Cas9 system, could have potential off-targets effects,<sup>27</sup> we carried out a BLAST analysis to predict potential off-targets, and we experimentally proved that *miniSINEUP-GDNF* showed no effects on these mRNAs.

We have also demonstrated that *in vivo* expression of *miniSINEUP-GDNF* RNA using an AAV9 is able to alter significantly the DA system's functions. In the striatum, we noted an increase in DA release using *in vivo* microdialysis after amphetamine infusion or potassium depolarization. Mice were also more sensitive to the locomotor effects induced by the systemic administration of amphetamine. Strikingly, DA storage pools were increased in striatal terminals by about 2-fold. It remains to be determined whether it is due to an increase in DA content in the surviving terminals or in the number of DA terminals in the striatum.

side effects caused by the ectopic GDNF overexpression were measured, the decrease in body weight (G) and the decrease in food intake (H). Mice injected with AAV9-*miniSINEUP-GDNF* did not show any side effect ( $n = 9$  for CTRL and 10 for *miniSINEUP-GDNF*). Data represent means  $\pm$  SEM. \* $p < 0.05$ , \*\* $p < 0.01$ , \*\*\* $p < 0.001$ . Unpaired t test with Welch's correction or repeated-measured ANOVA with Newman-Keuls test (C and D) was used.

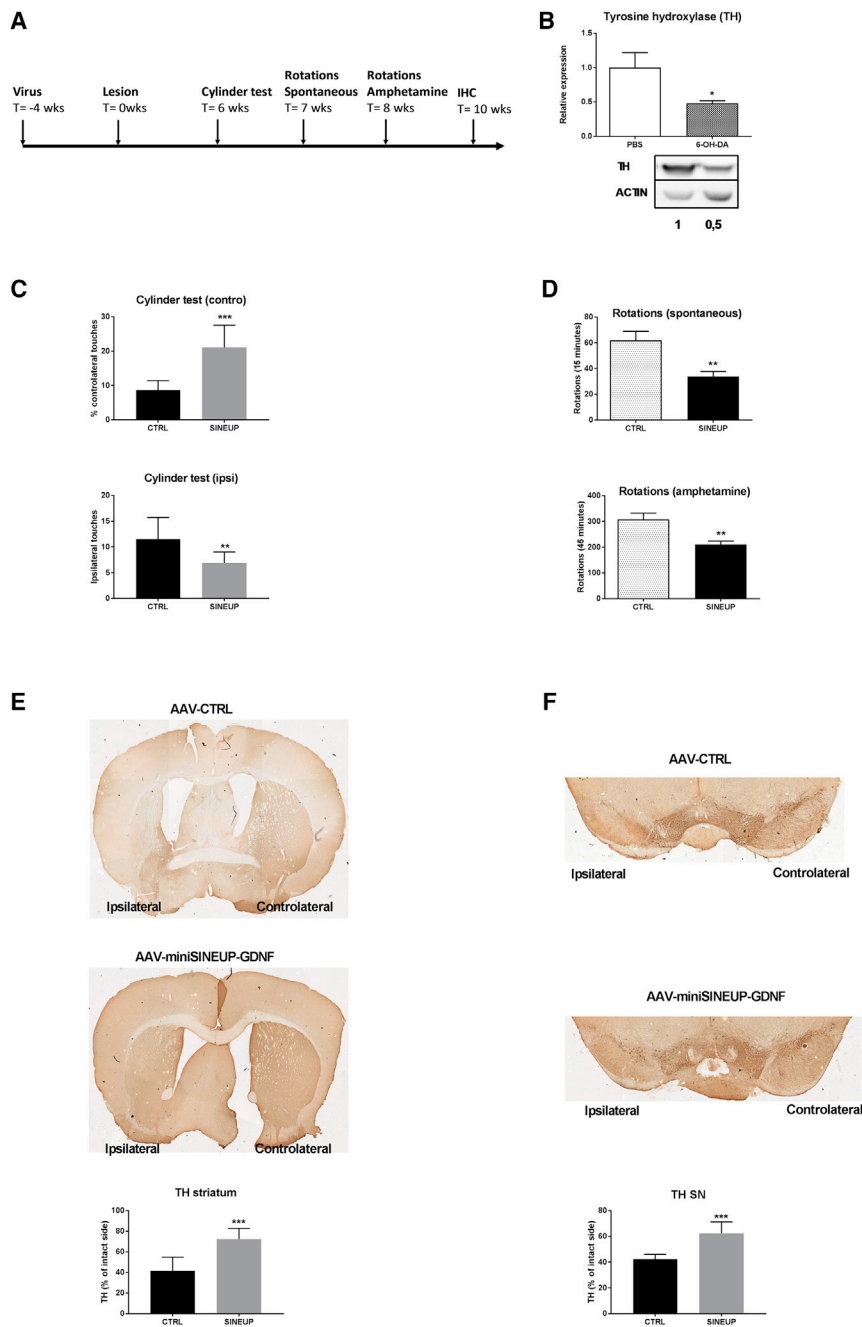


**Figure 4. *miniSINEUP-GDNF* RNA Rescues Neurodegeneration and Motor Phenotype in a PD Neurochemical PD Mouse Model**

(A) Scheme representing the experimental protocol used for the assessment of the neuroprotective effect of *miniSINEUP-GDNF*. AAV9 expressing *miniSINEUP-GDNF* was injected 4 weeks before the lesion, then 6, 7, and 8 weeks after the lesion behavioral tests were performed to verify the locomotor performance of mice. (B) Striatal lesion after 6-OHDA infusion was measured by TH quantification by western blot. Lesioned animals revealed a decrease in TH levels of approximately 50% ( $n = 5$ ). (C) The severity of the lesion was measured by the counting of the ipsilateral rotations of the lesioned mice. Both spontaneous rotations and the amphetamine-induced rotations were scored. For spontaneous rotations, videos were recorded for 15 min, while, for amphetamine-induced rotations, videos were recorded for 45 min ( $n = 9$ /group). (D) To assess the severity of the lesion, the cylinder test was carried out, where animals were scored for the contralateral forepaw usage. Ipsilateral touches were also counted ( $n = 9$ /group). (E) TH immunoreactivity of the striatum was evaluated by immunohistochemistry in mice injected with AAV9-*miniSINEUP-GDNF* or CTRL virus. Representative images of the striatum of *miniSINEUP* and CTRL animals are shown (upper panel). Quantification of the TH immunoreactivity was calculated for all animals (lower panel) ( $n = 9$ /group). (F) TH-positive neurons of the SNpc were evaluated by immunohistochemistry in mice injected with AAV9-*miniSINEUP-GDNF* or CTRL virus. Representative images of the SNpc of *miniSINEUP* and CTRL animals are shown (upper panel). Quantification of the TH-positive neurons was calculated for all animals (lower panel) ( $n = 9$ /group). Data represent means  $\pm$  SEM. \* $p < 0.05$ , \*\* $p < 0.01$ , \*\*\* $p < 0.001$ . Unpaired t test with Welch's correction was used.

More importantly, *miniSINEUP-GDNF* was able to ameliorate PD symptoms in the 6-OHDA PD mouse model. We used two behavioral assays widely used to assess the motor performance in this PD mouse model, the cylinder test and the rotational behavior. Mice injected with AAV9 expressing *miniSINEUP-GDNF* showed an improvement in the usage of the contralateral forepaw and significantly decreased the ipsilateral rotations. These data demonstrated an improvement in the motor behavior, the core symptomatology of PD. By analyzing TH immunoreactivity in the striatum and by counting DA neurons in the SNpc, we also demonstrated that *miniSINEUP-GDNF* could decrease DA loss induced by the 6-OHDA toxin infusion.

Interestingly, we did not observe any of the side effects caused by the GDNF ectopic overexpression, such as decreases in body weight and food intake. This is in line with our hypothesis that a moderate induction of GDNF expression in the correct cells, as mediated by SINEUP RNA activity, could be beneficial as a standard gene therapy approach but with less side effects. It should be noted that a more comprehensive study on the consequences of the ectopic expression of *SINEUP-GDNF* in other brain areas, including SNpc, will provide additional information on this important issue.

A limitation of this study is that there could be a difference in efficacy and in off-targeting of this approach between PD rodent models and humans. Studies in higher species such as non-human primates are, therefore, needed to validate SINEUP efficacy *in vivo*. Furthermore, it is well known that single PD mouse models are not reflecting the

complexity of the human pathology. Therefore, in addition to neurochemical intoxication, *miniSINEUP-GDNF* should be tested in other PD animal models, including those based on alpha-synuclein dysfunction. Importantly, while in this study RNA was expressed before lesioning the striatum (neuroprotection), for a clinical perspective, *miniSINEUP-GDNF* activity should be evaluated when the brain is lesioned before the delivery of the neurorestorative agent. There are other technologies that can increase the endogenous expression of selected genes, for example, zinc-finger-based artificial transcription factors<sup>28</sup> and CRISPR-based activation system (CRISPRa).<sup>29</sup> Both methods rely on the ability to stimulate transcription of a selected gene by activating its promoter. Potential advantages of SINEUPs over these technologies comprise SINEUPs work only when the target mRNA is expressed and the induction is within physiological levels.

There are several examples in the literature of long-term expression of transgenes in the human brain with AAV vectors.<sup>30,31</sup> An alternative strategy should be based on SINEUPs delivered as chemically synthesized nucleic acids by, i.e., intrathecal injection. In this context, we are focusing our efforts in decreasing the length of an active SINEUP. While the original AS Uchl1 RNA was larger than 1 kb, a miniSINEUP is around 250 nt long. A recent study of the structure of the invSINEB2 element acting as the ED in AS Uchl1 has shown the importance of Stem Loop 1 for SINEUP activity, prompting the synthesis of shorter active ED variants.<sup>32</sup>

In summary, our study has demonstrated that SINEUPs are an innovative technology to selectively increase the expression of target mRNAs *in vivo* in a physiological and specific manner, representing a new platform for gene therapy of neurodegenerative diseases.

## MATERIALS AND METHODS

### Construct

*miniSINEUP-GDNF* was generated by using the SINEUP-DJ1 as backbone.<sup>16</sup> BDs were designed in antisense orientation to the two most expressed isoforms targeting the first AUG, with a long (−40/+4) and a short (−14/+4) overlapping region. Oligonucleotides were annealed and cloned into recipient pCS2 plasmid. For doxocycline experiments, *miniSINEUP-GDNF* was cloned into a pLVX-TetOn-puro vector. AAV-*miniSINEUP-GDNF* was generated modifying an existing pAAV-CAG-EGFP vector (Addgene, 28014) by inserting between the intron and the GFP a sequence coding for the *miniSINEUP-GDNF*, a polyA signal, and a PGK promoter. This modification led us to have the *miniSINEUP-GDNF* expressed by the CAG promoter and the GFP expressed under the PGK promoter.

### Cell Lines and Transfection

Neuro2a and C8-D1A astrocyte type I clone were obtained from ATCC (Cat. No. CCL-131 and CRL-2541) and maintained in culture with DMEM (Gibco by Life Technologies, Cat. No. 41090-028) supplemented with 10% fetal bovine serum and 1% antibiotics (penicillin/streptomycin). Neuro2a and C8-D1A cells were plated in 6-well plates the day before transfection at 60% confluency ( $4 \times 10^5$  cells/well) and transfected with 1  $\mu$ g SINEUPs encoding plasmids using Lipofect-

amine 2000 (Invitrogen by Life Technologies, Cat. No. 11668019), following the manufacturer's instructions. Cells were collected 48 h after transfection. RNA and protein were obtained from the same transfection in each replica. For doxocycline induction experiments, Neuro2a was transfected with the pLVX-TetOn-puro vector expressing the *miniSINEUP-GDNF* and after 24 h doxocycline was added to the medium. At 24 h after doxocycline, cells were harvested and RNA and proteins were extracted. For the quantification of the GDNF in the medium, a kit from Abcam (ab171178) was used according to the manufacturer's instructions.

### RNA Extraction and qRT-PCR

Total RNA was extracted from cell pellets using TRIzol Reagent (Thermo Fisher Scientific, Cat. No. 15596026) and following the manufacturer's instructions. RNA samples were subjected to DNase (Sigma-Aldrich, Cat. No. AMPD1) treatment to avoid plasmid DNA contamination. A total of 1  $\mu$ g RNA was subjected to retrotranscription using iScriptcDNA Synthesis Kit (Bio-Rad, Cat. No. 1708890), according to the manufacturer's instructions. qRT-PCR was carried out using SYBR green fluorescent dye (SsoAdvanced Universal SYBR Green Supermix, Bio-Rad, Cat. No. 1725271) and an CFX96 Real time PCR System (Bio-Rad). The reactions were performed on diluted cDNA (1:8). Mouse glyceraldehyde 3-phosphate dehydrogenase (GAPDH) was used as the normalizing control in all qRT-PCR experiments. The amplified transcripts were quantified using the comparative Ct method, and the differences in gene expression were presented as normalized fold expression with the  $\Delta\Delta C_t$  method.

### Western Blot

Centrifuged cells or striatum from mice were lysed in radioimmunoprecipitation assay (RIPA) buffer with the addition of protease inhibitor cocktail (Sigma-Aldrich, Cat. No. P83490) buffer, briefly sonicated, and boiled for 5 min at 95°C. 30  $\mu$ g protein extracts were resolved by 4%–12% SDS-PAGE gels and transferred to 0.2  $\mu$ M nitrocellulose membrane (Amersham, Cat. No. GEH10600001) for 2 h at 35 V. Membranes were blocked with 5% non-fat dry milk in PBS/0.1% Tween 20 and incubated with the following indicated primary and secondary antibodies: anti- $\beta$ -actin 1:20,000 (Sigma, Cat. No. A2066), anti-GDNF 1:500 (Santa Cruz Biotechnology, Cat. No. sc-328), anti-TH 1:1,000 (Millipore, Cat. No. AB152), anti-DAD1 1:1,000 (Novus Biologicals, Cat. No. NB600-669), anti-LRRC14 1:1,000 (Novus Biologicals, Cat. No. NBP1-80049), and anti-CBX4 1:500 (Santa Cruz Biotechnology, Cat. No. sc-517216). The antibody against GDNF detects the mature form of GDNF, with an apparent molecular weight of approximately 17 kDa. Proteins of interest were visualized with the Amersham ECL Detection Reagents (GE Healthcare by Sigma, Cat. No. RPN2105). Western blotting images were acquired with Image Quant LAS 4000mini system, and band intensity was calculated using Image Quant TL software.

### Stereotaxic AAV9 and 6-OHDA Injection

The animals were anesthetized by a mixture of isoflurane/oxygen (1.5% of isoflurane during anesthesia with 1 L/min oxygen) and



placed on a stereotaxic apparatus (David Kopf Instrument, Tujunga, CA, USA) with mouse adaptor and lateral ear bars. The skin on the skull was cut and one hole was made on the same side by a surgical drill. AAV9-SINEUP (titer  $7.0 \times 10^{12}$  vg/mL) or AAV9-CTRL (titer  $7.0 \times 10^{12}$  vg/mL) was injected 1 month before the lesion in order to get the expression of the transgene. 1  $\mu$ L virus was injected in the right striatum at these coordinates: anteroposterior (AP) 0.5, dorsoventral (DV)  $-3.0$ , and lateral (L) 2.0. The virus was injected using a glass pipette and the rate of infusion was of 1  $\mu$ L/15 min. After the infusion, the pipette was maintained for another 5 min in the same position and then retracted slowly. At 4 weeks after the virus injection, all the animals received a stereotaxic injection of 6-OHDA or PBS at the same coordinates. 6-OHDA was dissolved in ascorbate-CNS Fluid 0.02% at a concentration of 4  $\mu$ g/ $\mu$ L and the volume administered was 2  $\mu$ L. All the animals received a desipramine 35 mg/kg injection (intraperitoneally [i.p.], dissolved in saline) to protect the noradrenergic innervations into the striatum. Sham-lesioned mice were injected with 0.02% ascorbate-saline devoid of 6-OHDA.

#### Behavioral Testing

All procedures involving animals and their care were carried out in accordance with the guidelines established by the European Community Council (Directive 2010/63/EU of September 22, 2010) and were approved by the Italian Ministry of Health (DL 116/92 and DL 111/94-B).

#### Locomotor Activity

To measure spontaneous locomotor activity, WT mice injected with AAV9 were placed in the locomotor activity chambers (Omnitech Digiscan, Accuscan Instruments, Columbus, OH, USA) for 60 min, and total distance traveled was measured by analyzing infrared beam interruptions. For amphetamine experiments, mice were habituated for 30 min in the apparatus and then injected i.p. with 2.5 mg/kg amphetamine (Sigma-Aldrich), and the distance traveled was measured for another 60 min.

#### Cylinder Test

During this test, animals were allowed to freely move in a clear glass cylinder for 5 min. A video camera was placed above the cylinder in order to see all the paw placements during the recording. An observer blinded to the animal treatment group viewed the recording and counted all the forepaw touches to the cylinder. The data were expressed as the percentage of contralateral touches.

#### Rotations

Spontaneous rotations were recorded 7 weeks after the lesion, while amphetamine-induced rotations were recorded 8 weeks after the lesion. Animals were placed in a glass cylinder 20 cm in diameter, and the rotational behavior was video recorded. For spontaneous rotation, mice were monitored for 15 min. For amphetamine-induced rotation, mice were injected i.p. with amphetamine at the dose of 2.5 mg/kg, and then animals were monitored for 45 min. Rotations were expressed as full 360° ipsilateral rotations.

#### Perfusion and Tissue Processing

Mice were deeply anesthetized with urethane (50 mg/kg, 10 mL/kg body weight, i.p., Sigma-Aldrich) and perfusion fixed by 10 mL 0.1 M phosphate buffer (pH 7.4) followed by 20 mL 4% formaldehyde. Brains were rapidly extracted and post-fixed in the same solution for 12 h at 4°C, and then cryoprotected in 30% sucrose in 0.1 M phosphate buffer (pH 7.4) for 48 h at 4°C. Sections were cut at 40  $\mu$ m in the coronal plane on a freezing microtome from the front of the striatum to the end of the retrorubral field.

#### Immunohistochemistry for TH

The sections were rinsed three times in 0.1 M PBS (pH 7.6), contained 0.1% Triton X-100 between each incubation period. All sections were quenched with 3% H<sub>2</sub>O<sub>2</sub>/10% for 10 min, followed by several changes of buffer. As a blocking step, sections were then incubated in 7% normal goat serum and 0.1% Triton X-100 for 2 h at room temperature. This was followed by incubation in primary antibody diluted in 3% normal goat serum and 0.1% Triton X-100 at 4°C for 24 h. The antibody used was an anti-TH diluted 1:500 (AB-152, Millipore). After incubation with the primary antibody, sections were rinsed and then incubated for 2 h at room temperature with biotinylated secondary antibodies (anti-rabbit 1:1,000; Thermo Scientific) in the same buffer solution. The reaction was visualized with avidin-biotin-peroxidase complex (ABC-Elite, Vector Laboratories), using 3,3'-diaminobenzidine as a chromogen. Sections were mounted on super-frost ultra plus slides (Thermo Scientific), dehydrated in ascending alcohol concentrations, cleared in xylene, and coverslipped in dibutyl phthalate polystyrene xylen (DPX) mounting medium. All sections were analyzed in the same experiment to keep staining conditions constant.

#### SNpc Cell Counts

The number of TH-positive cells was determined by counting every fourth 40- $\mu$ m section, as previously described.<sup>33</sup> The delimitation between the ventral tegmental area and the SN was determined by using the medial terminal nucleus of the accessory optic tract as a landmark. The unlesioned side was used as a control for the percentage of remaining neurons in each group.

#### Striatal Fiber TH Densitometry

The optical densities of the TH immunoreactive fibers in the striatum were measured using the NIH ImageJ program. For each animal the optical density was measured at four rostrocaudal levels over the whole striatum. To estimate TH staining density, the optical density was corrected for non-specific background density, as measured from the corpus callosum in each section. Data were presented as the average of the four rostrocaudal slice levels expressed as a percentage of the intact side.

#### Statistical Analysis

In all experiments, the significance of differences between groups was evaluated by Student's t test, one-way ANOVA, or repeated-measures ANOVA.  $p < 0.05$  was considered significant. Quantitative data are presented as mean  $\pm$  SEM.

**Data Availability**

All data and materials are available upon request.

**SUPPLEMENTAL INFORMATION**

Supplemental Information can be found online at <https://doi.org/10.1016/j.ymthe.2019.08.005>.

**AUTHOR CONTRIBUTIONS**

S.E. designed and carried out the experiments, analyzed the data, and composed the manuscript. M.S. carried out experiments. D.D. designed SINEUPs and analyzed experiments. F. Managò analyzed dopamine content. M.M. performed *in vivo* microdialysis. A.C. constructed the viruses. P.C. analyzed the data and discussed experimental results. C.S. analyzed the data and discussed experimental results. F.P. analyzed *in vivo* dopamine content and designed behavioral experiments. F. Mingozzi and G.R. designed and produced the AAV vectors used in the study. S.Z. designed SINEUPs, analyzed the data, and discussed experimental results. S.G. conceived the project, designed the experiments, analyzed the data, and composed the manuscript. All authors contributed to this work, read the manuscript, and agreed to its contents.

**CONFLICTS OF INTEREST**

S.G., S.Z., and P.C. declare competing financial interests as co-founders and member of Transine Therapeutics. S.G., S.Z., and P.C. are named inventors in a patent issued by the United States Patent and Trademark Office on SINEUPs.

**ACKNOWLEDGMENTS**

We are indebted to all the members of the S.G. lab for thought-provoking discussions. We thank Eva Ferri and Alessandra Sanna for administrative support. We are grateful to Luisa Franco and Ilaria Zarnardi for experimental advice and Monica Morini for experimental assistance at the animal facility. This work has been funded by IIT intramural grants to S.G.

**REFERENCES**

- Meissner, W.G., Frasier, M., Gasser, T., Goetz, C.G., Lozano, A., Piccini, P., Obeso, J.A., Rascol, O., Schapira, A., Voon, V., et al. (2011). Priorities in Parkinson's disease research. *Nat. Rev. Drug Discov.* 10, 377–393.
- Obeso, J.A., Stamelou, M., Goetz, C.G., Poewe, W., Lang, A.E., Weintraub, D., Burn, D., Halliday, G.M., Bezard, E., Przedborski, S., et al. (2017). Past, present, and future of Parkinson's disease: A special essay on the 200th Anniversary of the Shaking Palsy. *Mov. Disord.* 32, 1264–1310.
- Nagatsua, T., and Sawadab, M. (2009). L-dopa therapy for Parkinson's disease: past, present, and future. *Parkinsonism Relat. Disord.* 15 (Suppl 1), S3–S8.
- Kordower, J.H., and Bjorklund, A. (2013). Trophic factor gene therapy for Parkinson's disease. *Mov. Disord.* 28, 96–109.
- Lin, L.F., Doherty, D.H., Lile, J.D., Bektesh, S., and Collins, F. (1993). GDNF: a glial cell line-derived neurotrophic factor for midbrain dopaminergic neurons. *Science* 260, 1130–1132.
- Tomac, A., Lindqvist, E., Lin, L.F., Ogren, S.O., Young, D., Hoffer, B.J., and Olson, L. (1995). Protection and repair of the nigrostriatal dopaminergic system by GDNF *in vivo*. *Nature* 373, 335–339.
- Gash, D.M., Zhang, Z., Ovadia, A., Cass, W.A., Yi, A., Simmerman, L., Russell, D., Martin, D., Lapchak, P.A., Collins, F., et al. (1996). Functional recovery in parkinsonian monkeys treated with GDNF. *Nature* 380, 252–255.
- Kirik, D., Rosenblad, C., and Bjorklund, A. (2000). Preservation of a functional nigrostriatal dopamine pathway by GDNF in the intrastriatal 6-OHDA lesion model depends on the site of administration of the trophic factor. *Eur. J. Neurosci.* 12, 3871–3882.
- Nutt, J.G., Burchiel, K.J., Comella, C.L., Jankovic, J., Lang, A.E., Laws, E.R., Jr., Lozano, A.M., Penn, R.D., Simpson, R.K., Jr., Stacy, M., and Wooten, G.F.; ICV GDNF Study Group. Implanted intracerebroventricular. Glial cell line-derived neurotrophic factor (2003). Randomized, double-blind trial of glial cell line-derived neurotrophic factor (GDNF) in PD. *Neurology* 60, 69–73.
- Gill, S.S., Patel, N.K., Hotton, G.R., O'Sullivan, K., McCarter, R., Bunnage, M., Brooks, D.J., Svendsen, C.N., and Heywood, P. (2003). Direct brain infusion of glial cell line-derived neurotrophic factor in Parkinson disease. *Nat. Med.* 9, 589–595.
- Lang, A.E., Gill, S., Patel, N.K., Lozano, A., Nutt, J.G., Penn, R., Brooks, D.J., Hotton, G., Moro, E., Heywood, P., et al. (2006). Randomized controlled trial of intraputamenal glial cell line-derived neurotrophic factor infusion in Parkinson disease. *Ann. Neurol.* 59, 459–466.
- Kumar, A., Kopra, J., Varendi, K., Porokuokka, L.L., Panhelainen, A., Kuure, S., Marshall, P., Karalija, N., Härmä, M.A., Vilenius, C., et al. (2015). GDNF Overexpression from the Native Locus Reveals its Role in the Nigrostriatal Dopaminergic System Function. *PLoS Genet.* 11, e1005710.
- Carrieri, C., Cimatti, L., Biagioli, M., Beugnet, A., Zucchelli, S., Fedele, S., Pesce, E., Ferrer, I., Collavin, L., Santoro, C., et al. (2012). Long non-coding antisense RNA controls Uchl1 translation through an embedded SINEB2 repeat. *Nature* 491, 454–457.
- Zucchelli, S., Cotella, D., Takahashi, H., Carrieri, C., Cimatti, L., Fasolo, F., Jones, M.H., Sblattero, D., Sanges, R., Santoro, C., et al. (2015). SINEUPs: A new class of natural and synthetic antisense long non-coding RNAs that activate translation. *RNA Biol.* 12, 771–779.
- Patrucco, L., Chiesa, A., Soluri, M.F., Fasolo, F., Takahashi, H., Carninci, P., Zucchelli, S., Santoro, C., Gustincich, S., Sblattero, D., and Cotella, D. (2015). Engineering mammalian cell factories with SINEUP noncoding RNAs to improve translation of secreted proteins. *Gene* 569, 287–293.
- Zucchelli, S., Fasolo, F., Russo, R., Cimatti, L., Patrucco, L., Takahashi, H., Jones, M.H., Santoro, C., Sblattero, D., Cotella, D., et al. (2015). SINEUPs are modular antisense long non-coding RNAs that increase synthesis of target proteins in cells. *Front. Cell. Neurosci.* 9, 174.
- Sasso, E., Latino, D., Froehlich, G., Succoio, M., Passariello, M., De Lorenzo, C., Nicosia, A., and Zambrano, N. (2018). A long non-coding SINEUP RNA boosts semi-stable production of fully human monoclonal antibodies in HEK293E cells. *MAbs* 10, 730–737.
- Indrieri, A., Grimaldi, C., Zucchelli, S., Tammaro, R., Gustincich, S., and Franco, B. (2016). Synthetic long non-coding RNAs [SINEUPs] rescue defective gene expression *in vivo*. *Sci. Rep.* 6, 27315.
- Forrest, A.R., Kawaji, H., Rehli, M., Baillie, J.K., de Hoon, M.J., Haberle, V., Lassmann, T., Kulakovskiy, I.V., Lizio, M., Itoh, M., et al.; FANTOM Consortium and the RIKEN PMI and CLST (DGT) (2014). A promoter-level mammalian expression atlas. *Nature* 507, 462–470.
- Severin, J., Lizio, M., Harshbarger, J., Kawaji, H., Daub, C.O., Hayashizaki, Y., Bertin, N., and Forrest, A.R.; FANTOM Consortium (2014). Interactive visualization and analysis of large-scale sequencing datasets using ZENBU. *Nat. Biotechnol.* 32, 217–219.
- Modarresi, F., Faghihi, M.A., Lopez-Toledano, M.A., Fatemi, R.P., Magistri, M., Brothers, S.P., van der Brug, M.P., and Wahlestedt, C. (2012). Inhibition of natural antisense transcripts *in vivo* results in gene-specific transcriptional upregulation. *Nat. Biotechnol.* 30, 453–459.
- Ibáñez, C.F., and Andressoo, J.O. (2017). Biology of GDNF and its receptors - Relevance for disorders of the central nervous system. *Neurobiol. Dis.* 97 (Pt B), 80–89.
- Sullenger, B.A., and Nair, S. (2016). From the RNA world to the clinic. *Science* 352, 1417–1420.

24. Li, Z., and Rana, T.M. (2014). Therapeutic targeting of microRNAs: current status and future challenges. *Nat. Rev. Drug Discov.* *13*, 622–638.
25. Faghihi, M.A., Kocerha, J., Modarresi, F., Engström, P.G., Chalk, A.M., Brothers, S.P., Koesema, E., St Laurent, G., and Wahlestedt, C. (2010). RNAi screen indicates widespread biological function for human natural antisense transcripts. *PLoS ONE* *5*, e13177.
26. Gustincich, S., Zucchelli, S., and Mallamaci, A. (2017). The Yin and Yang of nucleic acid-based therapy in the brain. *Prog. Neurobiol.* *155*, 194–211.
27. Anderson, K.R., Haessler, M., Watanabe, C., Janakiraman, V., Lund, J., Modrusan, Z., Stinson, J., Bei, Q., Buechler, A., Yu, C., et al. (2018). CRISPR off-target analysis in genetically engineered rats and mice. *Nat. Methods* *15*, 512–514.
28. Sera, T. (2009). Zinc-finger-based artificial transcription factors and their applications. *Adv. Drug Deliv. Rev.* *61*, 513–526.
29. Matharu, N., Rattanasopha, S., Tamura, S., Maliskova, L., Wang, Y., Bernard, A., Hardin, A., Eckalbar, W.L., Vaisse, C., and Ahituv, N. (2019). CRISPR-mediated activation of a promoter or enhancer rescues obesity caused by haploinsufficiency. *Science* *363*, eaau0629.
30. Deverman, B.E., Ravina, B.M., Bankiewicz, K.S., Paul, S.M., and Sah, D.W.Y. (2018). Gene therapy for neurological disorders: progress and prospects. *Nat. Rev. Drug Discov.* *17*, 767.
31. Evers, M.M., Miniarikova, J., Juhas, S., Vallès, A., Bohuslavova, B., Juhasova, J., Skalnikova, H.K., Vodicka, P., Valekova, I., Brouwers, C., et al. (2018). AAV5-miHTT Gene Therapy Demonstrates Broad Distribution and Strong Human Mutant Huntingtin Lowering in a Huntington's Disease Minipig Model. *Mol. Ther.* *26*, 2163–2177.
32. Podbevšek, P., Fasolo, F., Bon, C., Cimatti, L., Reißer, S., Carninci, P., Bussi, G., Zucchelli, S., Plavec, J., and Gustincich, S. (2018). Structural determinants of the SINE B2 element embedded in the long non-coding RNA activator of translation AS Uchl1. *Sci. Rep.* *8*, 3189.
33. Bensadoun, J.C., Déglon, N., Tseng, J.L., Ridet, J.L., Zurn, A.D., and Aebischer, P. (2000). Lentiviral vectors as a gene delivery system in the mouse midbrain: cellular and behavioral improvements in a 6-OHDA model of Parkinson's disease using GDNF. *Exp. Neurol.* *164*, 15–24.